Nanoscale Advances

ROYAL SOCIETY OF CHEMISTRY

PAPER

View Article Online
View Journal | View Issue

Cite this: *Nanoscale Adv.*, 2021, **3**, 1087

Preparation of Cu cluster catalysts by simultaneous cooling–microwave heating: application in radical cascade annulation†

Liangliang Song,‡[a] Roberta Manno,‡[bc] Prabhat Ranjan,[a] Victor Sebastian, *[bcd] Silvia Irusta,[bcd] Reyes Mallada,[bcd] Luc Van Meervelt,[e] Jesús Santamaria[bcd] and Erik V. Van der Eycken *[af]

One of the hallmarks of microwave irradiation is its selective heating mechanism. In the past 30 years, alternative designs of chemical reactors have been introduced, where the microwave (MW) absorber occupies a limited reactor volume but the surrounding environment is MW transparent. This advantage results in a different heating profile or even the possibility to quickly cool down the system. Simultaneous cooling–microwave heating has been largely adopted for organic chemical transformations. However, to the best of our knowledge there are no reports of its application in the field of nanocluster synthesis. In this work, we propose an innovative one-pot procedure for the synthesis of Cu nanoclusters. The cluster nucleation was selectively MW-activated inside the pores of a highly ordered mesoporous substrate. Once the nucleation event occurred, the crystallization reaction was instantaneously quenched, precluding the growth events and favoring the production of Cu clusters with a homogenous size distribution. Herein, we demonstrated that Cu nanoclusters could be successfully adopted for radical cascade annulations of *N*-alkoxybenzamides, resulting in various tricyclic and tetracyclic isoquinolones, which are widely present in lots of natural products and bioactive compounds. Compared to reported homogeneous methods, supported Cu nanoclusters provide a better platform for a green, sustainable and efficient heterogeneous approach for the synthesis of tricyclic and tetracyclic isoquinolones, avoiding a variety of toxic waste/byproducts and metal contamination in the final products.

Received 24th November 2020
Accepted 9th January 2021

DOI: 10.1039/d0na00980f

rsc.li/nanoscale-advances

Introduction

Over the past decade, metal nanoclusters (NCs) have attracted intense interest due to their use in different kinds of emerging technological applications, including catalysis, biology, and medicine.[1–6] As demonstrated by Nørskov *et al.*,[4b] in the nanocluster scale (diameter < 2 nm) the number of accessible active sites increases, and the majority of them will occupy edges or corners, which implies a different coordination number. Furthermore, the discretization of the electronic energy levels results in quantum size effects, losing the metallic behavior, still observed for crystalline nanoparticles.[5b,c] The catalytic activity of metallic clusters may be strongly enhanced as largely demonstrated for Au and Ag NCs, which have been proposed as valid alternatives to highly expensive metals, *i.e.* Pd or Pt.[7–10] Recently, Cu NCs begin to receive increasing attention and exhibit high potential for large-scale nanotechnology applications, not only due to their high yields in facile synthesis and impressive optical properties, but also due to the earth-abundance (around four orders of magnitude higher than Au, Ru or Pt)[11a] and low cost of Cu as well as its environmentally benign character.[11–17]

Despite extensive research investigations of Au and Ag NCs,[18–25] studies focusing on the synthesis of Cu NCs are scarce mainly due to the difficulty in synthesizing highly stable and small Cu(I)/Cu(0) nanomaterials.[26–31] For example, in 2009, Vázquez-Vázquez and co-workers prepared stable and small Cu NCs through the employment of a slow water-in-oil microemulsion technique.[29] Subsequently, Vilar-Vidal and co-

[a]*Laboratory for Organic & Microwave-Assisted Chemistry (LOMAC), Department of Chemistry, KU Leuven, Celestijnenlaan 200F, 3001, Leuven, Belgium. E-mail: erik.vandereycken@kuleuven.be*

[b]*Instituto de Nanociencia y Materiales de Aragón (INMA), CSIC-Universidad de Zaragoza, Zaragoza 50009, Spain. E-mail: victorse@unizar.es*

[c]*Department of Chemical & Environmental Engineering, Edificio I+D+i, Campus Rio Ebro, C/MarianoEsquillor s/n, 50018, Zaragoza, Spain*

[d]*Networking Research Center CIBER-BBN, 28029 Madrid, Spain*

[e]*Biomolecular Architecture, Department of Chemistry, KU Leuven, Celestijnenlaan 200F, 3001, Leuven, Belgium*

[f]*Peoples' Friendship University of Russia (RUDN University), Miklukho-Maklaya Street 6, Moscow, 117198, Russia*

† Electronic supplementary information (ESI) available. See DOI: 10.1039/d0na00980f

‡ These authors contributed equally to this work.

workers[31] synthesized aggregates of stable and small Cu_n NCs ($n \leq 14$) in aqueous solution *via* a simple electrochemical cycle of 1000 s. Even if every single cluster presented a diameter smaller of (0.61 ± 0.13) nm, the XPS analysis confirmed that the aggregates presented a core–shell structure, with a thin layer of Cu(II) ions over the external surface. Recently, Kawasaki's group[30] reported the synthesis of approximately 2 nm Cu NCs without using additional protective and reducing agents by using a microwave-assisted polyol method. Cu(I)/Cu(0) nanoparticles of (2.3 ± 0.3) nm were obtained after 30 min of MW irradiation achieving a maximum synthesis temperature of 185 °C in inert atmosphere.

As reported in our previous work,[32a] microwave irradiation may guarantee a heating rate 10 times higher than conventional heating. This promotes a nearly instantaneous and homogeneous nucleation. However, in accordance with the LaMer model,[32b] the initial nuclei are unstable and tend to aggregate, generating bigger nanoparticles. The rapid quenching of the reaction and the heterogenization of the nanoclusters may guarantee a longer stability.[32c–e]

Herein, we present an innovative microwave heating reactor, cooled by ice to preclude the growth of nanoclusters and to avoid MW absorption, for the *in situ* production of Cu NCs directly inside of the 10 nm diameter channels of ordered SBA-15 nanorods. The nanosynthesis reactor was designed exploiting the selectivity of microwave heating. The dielectric loss tangent $\tan\delta = \varepsilon''/\varepsilon'$, defined as the ratio between the dissipated energy (ε'') and the energy stored (ε'),[33a] describes the interaction of each material with the electromagnetic wave (Table 1). On the basis of its value, we can distinguish between reflectors (*e.g.* metals), transmitters ($\tan\delta < 0.1$, *e.g.* quartz or Teflon®) and absorbers ($\tan\delta > 0.1$).[33b] In this work, the water based precursors behave as high microwave absorbers. On the other hand, the reactor was surrounded by a thin layer of water ice, conferring microwave transparency.[33c] In this way, a simultaneous cooling–microwave heating occurred, guaranteeing both a rapid localized nucleation and a nearly instantaneous blocking of undesired aggregation events.

Polycyclic isoquinolone frameworks are widely present in lots of natural products and bioactive compounds,[34,35] such as naturally occurring alkaloids, industrially employed dyes, paints, insecticides, antifungals, anesthetics, antihypertension agents, disinfectants, and vasodilators.[35b] Although several efficient methods have been developed to synthesize these scaffolds, they mainly focus on homogeneous catalytic conditions, including transition metal-catalyzed cascade annulation reactions.[36–43] They have to utilize highly toxic, hazardous and expensive chemicals, and inevitably lead to a number of toxic waste/byproducts and metal contamination in the final products. Therefore, developing a green, sustainable and efficient approach for the construction of polycyclic isoquinolones still remains a challenging task.

Despite the broad scope of diverse organic transformations by Cu nanoparticles (NPs),[44] organic synthesis employing Cu NCs has been scarcely studied.[45,46] Most examples of Cu NCs focused on galvanic reactions, hydrogen evolution reactions, reduction of CO_2 and fluorescence properties.[11–17] Considering the excellent performance of Cu catalysts in homogeneous radical reactions,[47] we next evaluated the catalytic activity of Cu-NCs@SBA-15, unveiling their influence on the activity and selectivity towards isoquinolones and exploiting their unprecedented catalytic properties.

The catalytic activity of supported Cu-NCs@SBA-15 catalyst was successfully illustrated by the further radical cascade annulations of *N*-alkoxybenzamides for the construction of various tricyclic and tetracyclic isoquinolones. This heterogeneous catalyst is stable and reusable under the employed reaction conditions and can be easily isolated. To the best of our knowledge, this is the first report on Cu NCs exhibiting such remarkable activity to radical cascade annulation reaction.

Experimental

Synthesis of amine grafted SBA-15

The mesoporous SBA-15 nanorods were synthesized by a traditional sol–gel procedure.[48] The non-ionic surfactant Pluronic P-123 (1.2 g) was dissolved into 40 mL of HCl 1.75 M (AnalaR NORMAPUR 37%) with the addition of 14 mg of ammonium fluoride NH_4F (Sigma Aldrich, ≥98%). In this step the reactor volume was strictly maintained at 20 °C and 1500 rpm stirring rate (magnetic stirrer bar of Ø 6 mm × 25 mm) for 4 h. Then, a fresh mixture of heptane (Sigma-Aldrich, 99% – 8.5 mL) and TEOS (Fluka, 98% – 2.75 mL) was added, keeping the reaction at 1500 rpm stirring rate for 4 min. The heptane acts as swelling agent,[49] guaranteeing a higher final pore diameter.[50] After 10 min in a static condition, the solution was transferred to a PTFE-lined autoclave for hydrothermal treatment at 100 °C for

Table 1 Loss tangent and penetration depth of materials employed for the reactor design[33c,51]

Material	Loss tangent δ	Penetration depth (mm)
(1) Teflon®	0.00028	92 000
(2) Ice	0.0009	11 000
(3) Pyrex	0.0005	~10 000
(4) Water	0.157	14

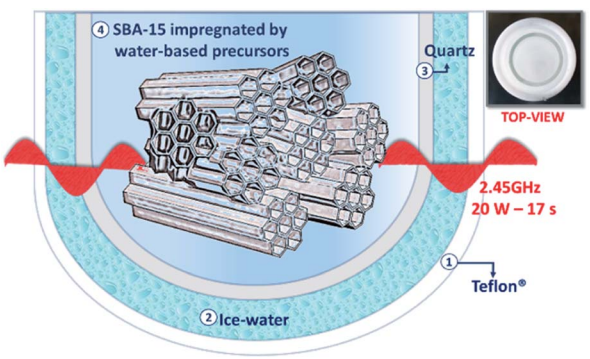

Fig. 1 Schematic representation and optical inset of the coaxial reactor for the simultaneous cooling–microwave heating.

24 h. Next, the product was washed, filtered and calcined in a muffle furnace at 550 °C for 5 h with a heating rate of 1 °C min^{-1}. To conclude, the empty rod-shaped channels of SBA-15 were amino-functionalized according to a previously described procedure.[32e] A mass of 1 g of calcined rod-shape SBA-15 was dispersed into 20 mL of toluene (Fisher Chemical, General Purpose Grade). After 15 min of Ar-purging, we added 400 μL of (3-aminopropyl)triethoxysilane (Sigma-Aldrich, ≥98%) maintaining the system at 110 °C for 1 h. Finally, the product was filtered, washed with a mixture of dichloromethane/diethyl ether (1 : 1 in volume) and dried at 80 °C overnight.

Synthesis of Cu nanoclusters

To prepare Cu nanoclusters we employed the reactor schematically represented in Fig. 1, which consisted of two coaxial tubes. The external one (O.D. 24.5 mm, I.D. 20.7 mm) was made of Teflon, while the internal one was made of Pyrex (O.D. 16.4 mm, I.D. 13.3 mm). The interspace between them was occupied by ice. As reported in Table 1, Teflon®, Ice and Pyrex are microwave transparent materials. On the contrary the liquid water is a good MW absorber. The reactor was fixed in the centre of a monomode CEM Discover® cavity immediately before starting the synthesis. 5 mg of $Cu(NO_3)_2 \cdot 3H_2O$ (Sigma-Aldrich) were dissolved in 400 μL of deionized water with the addition of 123 μL of Na-PAA (Sigma Aldrich MW 1200, 45 wt% in water). Then, 100 mg of amino-functionalized SBA-15 was loaded in the central volume and impregnated by the water-based copper precursors to incipient wetness. After homogenisation for 30 s by vigorous stirring, the sample was irradiated by MWs-20 W for 17 s in high stirring condition. Once the microwaves were switched-off, the ice rapidly cooled-down the system. To conclude, the catalyst was purified by centrifugation at 12 000 rpm for 20 min with distilled water and dried at 50 °C overnight.

Characterization techniques

High-angle annular dark-field scanning transmission electron microscope (HAADF-STEM) FEI Titan™ (80–300 kV) and elemental analysis carried out with an EDS detector performed in the scanning mode were adopted to confirm that the NCs were smaller than 2 nm and were homogeneously distributed over the mesoporous substrate. A 10 μL drop of Cu-NCs@SBA-15 catalyst was dispersed in water, sonicated for 30 s and deposited onto a holey carbon grid, made of Ni.

For heterogeneous catalysis it is important to verify that the porous channels are not obstructed and the pores diameter is big enough to assure the entrance and diffusion of the organic substrate. The pore size distribution analysis was performed by nitrogen adsorption at 77 K in a Micrometrics ASAP 2020, outgassing the sample at 26.7 Pa and 383 K for 5 h. The Brunauer–Joyner–Halenda (BJH) method was applied to the adsorption branch to calculate mean pore diameter (MPD) and pore size distribution. The Brunauer–Emmett–Teller (BET) method was applied to the adsorption isotherm in the range of relative pressure 0.06–0.19 to calculate specific surface area.

The quantification of the Cu metal loading of the fresh catalyst and after 3rd reaction cycle was conducted by Microwave Plasma Atomic Emission Spectroscopy (MP-AES) (Agilent 4100 MP-AES). First, 30 mg of the catalyst were digested under microwave heating (200 °C for 20 min in Milestone Ethos Plus microwave cavity) in 5 mL of a mixture of nitric acid (HNO_3) and hydrochloric acid (HCl) in a volume ratio of 1 : 3. Afterward, the sample was five times diluted by Milli-Q-water and filtered by hydrophilic syringe filters of 0.2 μm. Finally, we determined the oxidation state of Cu NCs before and after catalytic test, using X-ray photoelectron spectroscopy (XPS, Axis Supra spectrometer – Kratos Tech). The samples were excited by a monochromatized Al Kα source at 1486.6 eV, run at 12 kV and 10 mA. A survey spectrum was measured at 160 eV pass energy, for the individual peak regions, spectra were recorded with a pass energy of 20 eV. The peaks were studied by CasaXPS software, adopting a weighted sum of Lorentzian and Gaussian component curves after Shirley background subtraction. The binding energies were referenced to the internal C1s standard at 284.9 eV.

Catalytic activity

To a Schlenk flask equipped with a stir bar were added **1** (0.1 mmol), Cu NCs (5 mol%), *t*BuOOH (50 mol%) and 1,4-dioxane (1.0 mL) without any particular precautions to remove oxygen or moisture. The reaction vial was immersed in an oil bath pre-heated at 100 °C and stirred at 800 rpm. After 20 h, the reaction mixture was centrifuged and the catalyst was washed three times with 1,4-dioxane. The resulting organic layer was evaporated under reduced pressure, and the residue was purified by silica gel column chromatography (*n*-heptane/ethyl acetate from 2 : 1 to 1 : 2). The obtained products were characterized by ^1H and ^{13}C NMR spectroscopy as well as HRMS (see ESI†).

Reusability test

To a Schlenk flask equipped with a stir bar were added **1** (0.1 mmol), Cu NCs (5 mol%), *t*BuOOH (50 mol%) and 1,4-dioxane (1.0 mL) without any particular precautions to extrude oxygen or moisture. The reaction vial was immersed in an oil bath pre-heated at 100 °C and stirred at 800 rpm. After the 20 h, the reaction mixture was centrifuged and the catalyst was washed three times with 1,4-dioxane. The resulting organic layer was evaporated under reduced pressure, and the residue was purified by silica gel column chromatography. The catalyst was dried under vacuum oven at 50 °C for 24 h and used for another cycle.

Leaching test

Hot filtration test was performed to evaluate the stability of the catalyst towards leaching by removing the catalyst from the reaction mixture after 4 h. The reaction mixture was then transferred into a new reaction vial equipped with a new stirring bar and was continuously stirred for another 16 h at 100 °C. The reaction ceased after the removal of the catalyst from the reaction mixture and no further conversion was observed, supporting the heterogeneous nature of the reaction.

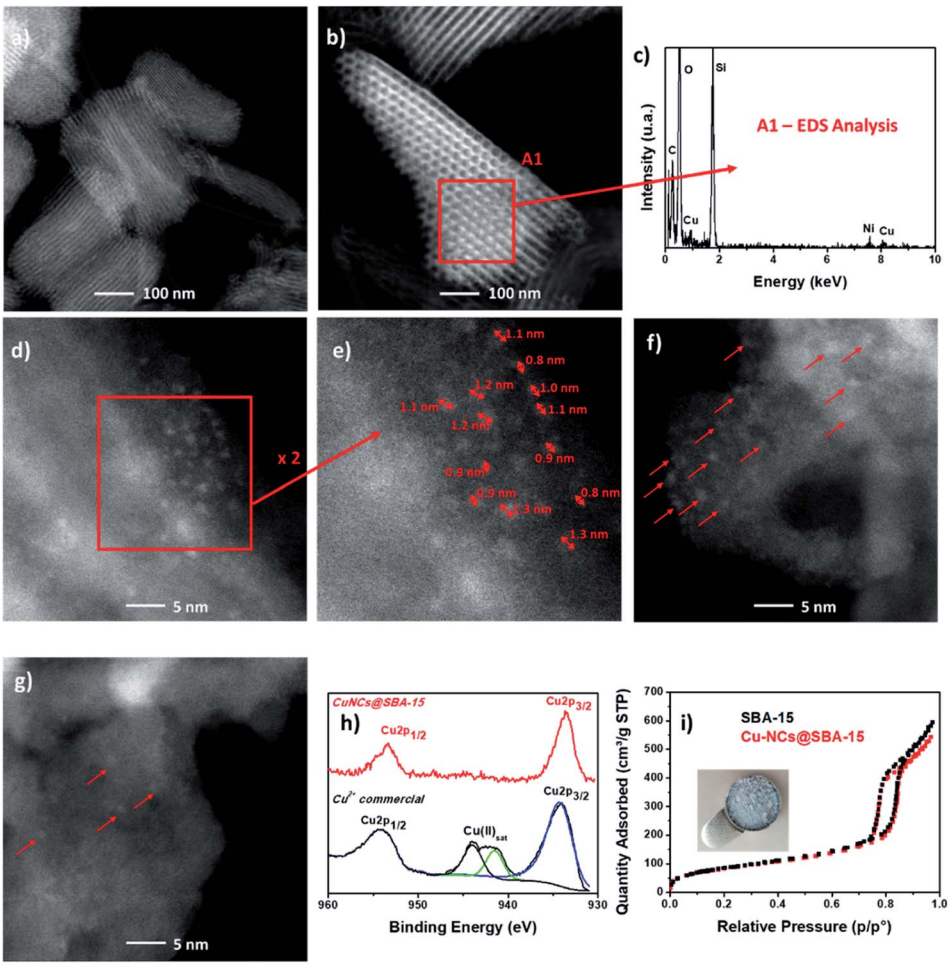

Fig. 2 (a and b) HAADF-HRSTEM analysis of Cu-NCs@SBA-15 with the selection of an area of 4 μm^2 and (c) its relative EDS analysis. (d–g) HAADF-HRSTEM analysis of Cu-NCs smaller than 2 nm. (h) Cu 2p XPS core level of Cu-NCs@SBA-15 in red and Cu(II) pattern in black showing the characteristic satellite peaks. (i) N_2 adsorption curve for the mesoporous substrate and the Cu-NC@SBA-15 catalyst.

Results and discussion

Synthesis of Cu-NCs/SBA-15

The control of the size distribution in supported nanoclusters is deemed important and it is still one the main challenges to achieve in catalysts production. In our work, no copper aggregation in form of nanostructures was observed by electron microscopy analysis (Fig. 2a and b). The detection of Cu clusters on SBA-15 functionalized surface was achieved using the HAADF detector, since the contrast is approximately proportional to the square of the atomic number of the elements. A thick area (SBA surface) with lighter elements (Si and C) might have the same contrast as a thinner area with heavier atoms (Cu NCs), making the identification of Cu metallic clusters from the mesoporous substrate more difficult. EDS analysis confirmed the presence of metallic Cu clusters over the analyzed surface of the mesoporous substrate (Fig. 2c). High-resolution imaging of the mesoporous channels, in Fig. 2d–g, evidenced the presence of Cu NCs smaller than 1.5 nm. Compared to literature data, the innovative procedure here described is free of toxic reagents, such as sodium borohydride largely adopted as reducing agent for template-assisted synthesis.[52] To balance the aggregation force during the synthesis of nanoclusters, traditional procedures usually adopt high concentration of long-chain organic molecules, guaranteeing a long-time stability but reducing the accessibility of reagents to the active sites for catalytic applications. In addition, the synthesis of unsupported nanoclusters hamper catalyst recovery and reusability.[53] On the other hand, *in situ* nucleation assures synthesis yield higher than 80%, but the long reaction times required (1–24 h)[54] lead to lack of control of size distribution. All of these problems hinder the scalability of the synthesis process from the laboratory scale. To address all these shortcomings, the proposed simultaneous cooling–microwave heating method allows the production of 100 mg of catalyst in less than 1 min per batch, with a final metal loading of (1.2 ± 0.2)%, corresponding to a synthesis yield of 71%, an intermediate position between methods based on wet-impregnation grafting, where yields are around 50%, and alternative *in situ* techniques such as H_2 cold plasma or solid grinding, which may guarantee a loading yield higher than 90%.[55] Therefore our proposed methodology is safe, efficient, atom economical, simple and suitable for large scale production. Furthermore, as is well known, Cu nanoparticles are usually oxidized in a rapid manner, resulting in a high

Table 2 N_2 adsorption measurement for SBA-15 and Cu-NCs@SBA-15

Sample	S_{BET} ($m^2\ g^{-1}$)	V_t ($cm^3\ g^{-1}$)	D_{BJH} (nm)
SBA-15	317	0.89	9.3
Cu-NCs@SBA-15	306	0.69	8.1

concentration of Cu(II)[56] over the external surface of the nanoparticle, a Cu(II) shell that is inactive for several chemical processes. As reported by Boronat *et al.*,[57] a low oxidation rate was observed for ultra-small nanoclusters. We confirmed by XPS (Fig. 2h), that the sub-1.5 nm Cu NCs synthesized, presented the oxidation states of Cu(0) and Cu(I), whose peaks cannot be separated. However, no satellite peak of Cu(II) was observed, as reported in Fig. 2h in red. This insight is in accordance with the recent results reported by Abiraman *et al.* of unsupported sub-1 nm Cu(I) NCs stabilized by PAA template.[58] The size control and uniformity achieved with this methodology is as good as the one reported with the template methodology,[59] but the size was significantly decreased when compared with the use of cysteamine,[60] DNA,[61] cisplatin[62] or BSA[63] as a template.

Finally, no pore obstruction occurred after Cu NCs grafting (Fig. 2i). As listed in Table 2, the pore volume and the surface S_{BET} decreased respectively of 22% and 3.5%. No relevant variation of the pore diameters occurred with a final diameter of 8.1 nm, which assured the accessibility of the mesoporous channels for heterogeneous catalytic applications.

Heterogeneously catalyzed reaction

Due to the number of broad biological applications of polycyclic isoquinolines, there is high interest to develop a green, sustainable and efficient approach for the production of polycyclic isoquinolones. In 2018, Han and co-workers reported a homogeneous Cu-catalyzed radical cascade annulation for the synthesis of 1,2-oxazinane-fused isoquinolin-1(2*H*)-ones in moderate to good yields, along with the unexpected oxygen-trapped spirocyclic byproducts.[47d] Based on this, we investigated the catalytic activity of the new Cu-NCs@SBA-15 in a cascade radical cyclization reaction. This reaction commenced by using **1a** as a model substrate to optimize the reaction conditions. When the reaction was performed with Cu NCs (5 mol%) in EtOAc at 100 °C for 12 h, the desired tetracyclic isoquinolone **2a** was isolated in 41% yield (Table 3, entry 1). The structure of **2a** was confirmed by X-ray diffraction. Then various solvents were screened, such as CH_3CN, MeOH, 1,4-dioxane, THF, 1,2-dichloroethane, acetone and toluene, showing that 1,4-dioxane and 1,2-dichloroethane could give better results (entries 2–8). A longer reaction time and a lower concentration gave some improvements (entries 9 and 10). When 50 mol% *t*BuOOH was used as additional oxidant, **2a** was obtained in 64% yield after 20 h (entry 11). Next Cu-NPs@SBA-15 (5 mol%) prepared by traditional impregnation method and CuCl (5 mol%) were respectively considered as heterogeneous and homogeneous catalysts[47d] to benchmark the heterogeneous reaction results. Nevertheless, both of them gave lower yields (entries 12 and 13) because of unidentified side products, indicating the high efficiency of our synthesized Cu NCs.

Two pathways are proposed for the radical cascade annulations (Scheme 1). Firstly, Cu(I) reacts with oxygen molecule from air to give Cu(II) intermediate **A** or **B**. Substrate **1a** is oxidized by **A** or **B** through a hydrogen atom transfer process to produce the Cu(II) intermediate **C** or **D** and radical intermediate **E** (path a). Alternatively, Cu(I) and TBHP undergo inner-sphere single-

Table 3 Optimization of the reaction conditions[a]

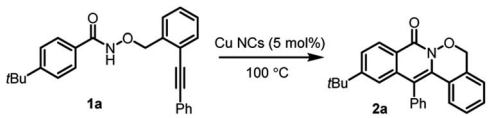

Entry	Solvent	t (h)	Yield[b] (%)
1	EtOAc (0.2 M)	12	41
2	CH_3CN (0.2 M)	12	52
3	MeOH (0.2 M)	12	4
4	1,4-Dioxane (0.2 M)	12	55
5	THF (0.2 M)	12	0
6	1,2-Dichloroethane (0.2 M)	12	56
7	Acetone (0.2 M)	12	0
8	Toluene (0.2 M)	12	18
9	1,4-Dioxane (0.2 M)	20	57
10	1,4-Dioxane (0.1 M)	20	58
11[c]	**1,4-Dioxane (0.1 M)**	**20**	**64**
12[c,d]	1,4-Dioxane (0.1 M)	20	52
13[c,e]	1,4-Dioxane (0.1 M)	20	54

[a] Conditions: **1a** (0.05 mmol), Cu NCs (5 mol%), solvent, 100 °C. [b] Isolated yield. [c] 50 mol% *t*BuOOH was added. [d] 5 mol% CuCl was added. [e] 5 mol% Cu-NPs@SBA-15 was added.

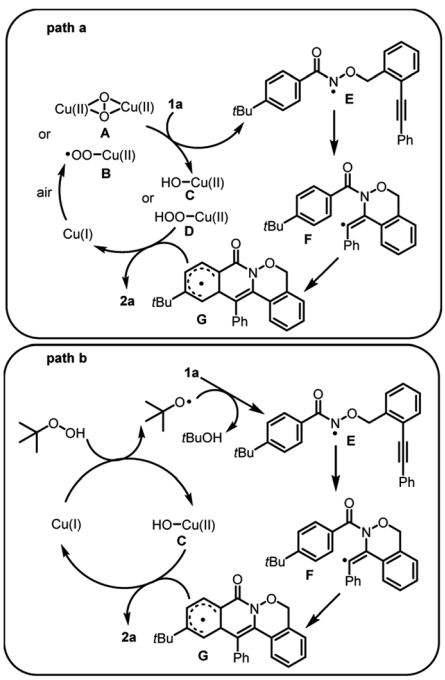

Scheme 1 Proposed mechanism.

Table 4 Catalyst activity test up to 3 cycles

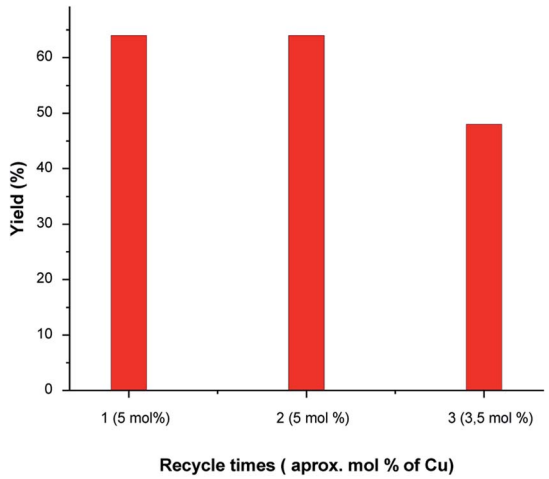

Table 5 Catalyst loading determination of fresh and used catalyst

	After synthesis	After 3rd cycle
Metal loading	(1.2 ± 0.2) wt%	(0.9 ± 0.1) wt%

electron transfer process to give Cu(II) species **C** and *t*BuO radical. Then *t*BuO radical obtains a hydrogen atom from substrate **1a** to afford radical intermediate **E** and *t*BuOH (path b). Then **E** undergoes intramolecular 6-*exo-dig* cyclization to deliver intermediate **F**. This is followed by aromatic homolytic substitution to afford intermediate **G**. Product **2a** is given from the aromatization of **G** and Cu(I) is regenerated from **C** or **D**.

In order to verify the stability of the new Cu NCs catalyst, the leaching behavior of the supported Cu NCs was firstly evaluated. First, we performed a hot-filtration test by filtering off the catalyst after 4 h under reaction conditions and did not detect further conversion after the removal of the catalyst, suggesting that the reaction is heterogeneous. We employed our catalyst up to 3 cycles (Table 4). After the 3rd cycle, we observed a slight decrease in the conversion. Agglomeration of nanoparticles is quite common at the higher temperature. To evaluate the deactivation of this catalyst after the 3rd catalytic cycle, we performed HRSTEM and XPS analyses. The stressed and prolonged high reaction temperature initiated undesired nanocluster aggregation, observing two different populations small clusters and particles whose diameter ranged between 2 and 3 nm, as reported in Fig. 3a–d. Moreover, a percentage of 29% of Cu(II) was determined by XPS after the 3rd catalytic cycle, as reported in Fig. 3e. The presence of Cu(II) can be rationalized by the proposed mechanisms. Furthermore, 25% of copper leaching was evidenced by the MP-AES analysis of the catalyst after 3rd catalytic cycle (Table 5). All these evidences support the decrease in the conversion after 3rd catalytic cycle.

With the optimal conditions in hand, various substrates were explored to evaluate the scope of the Cu NCs-catalyzed cascade radical cyclization (Table 6). The reaction was compatible with *N*-alkoxybenzamides bearing diverse electron-donating or electron-withdrawing groups at the *para* position of the benzamide moiety, resulting in the formation of

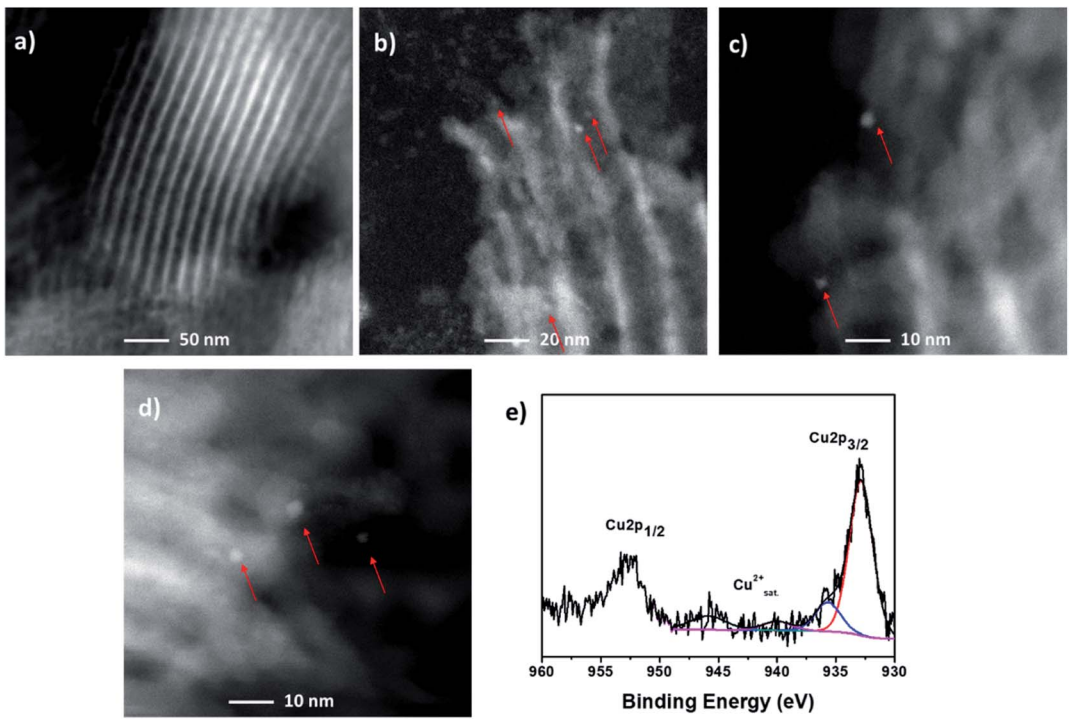

Fig. 3 (a–d) HAADF-HRSTEM analysis and (e) Cu 2p XPS spectrum of the heterogeneous catalyst after 3rd cycle at 100 °C for 20 h in 1,4-dioxane.

Table 6 Scope for *N*-alkoxybenzamide substrates[a,b]

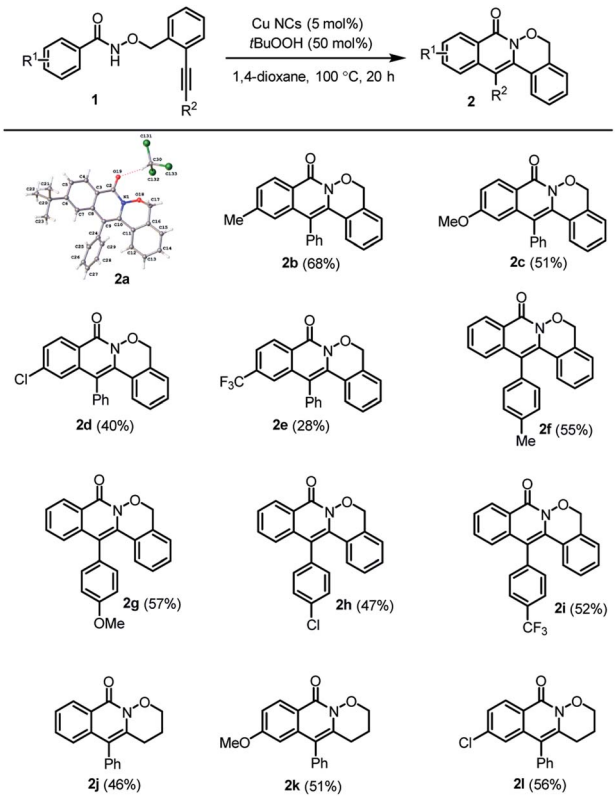

[a] Conditions: **1** (0.1 mmol), Cu NCs (5 mol%), *t*BuOOH (50 mol%), 1,4-dioxane (1.0 mL), 100 °C, 20 h. [b] Isolated yield.

tetracyclic isoquinolones **2b–e** in 28–68% yield. Substrates with various electron-donating or electron-withdrawing groups at the *para* position of the phenylacetylene part also proceeded smoothly to deliver the corresponding tetracyclic isoquinolones **2f–i** in 47–57% yield. Additionally, reactions bearing substrates with flexible tethers were tolerated, leading to the corresponding tricyclic isoquinolones **2j–l** in 46–56% yield. Notably, during the process of evaluating the scope, we did not observe the formation of unexpected oxygen-trapped spirocyclic byproducts,[47d] which indicates the excellent selectivity triggered by our prepared Cu NCs.

Conclusions

Simultaneous cooling–microwave heating is an efficient procedure for the synthesis of metallic nanoclusters. The sub-1.5 nm Cu clusters prepared in this work were homogeneously distributed on the ordered mesoporous SBA-15, avoiding undesired aggregations and pore obstruction. Furthermore, no Cu(II) impurities were observed in the prepared catalyst. The proposed methodology to produce Cu clusters-based catalyst is safe, efficient, atom economical, simple and suitable for large scale production. The catalyst was efficiently applied in the production of the highly demanded tricyclic and tetracyclic isoquinolones by radical cascade annulations of *N*-alkoxybenzamides. Compared to conventional homogeneous strategies, supported Cu nanoclusters set the better stage for green, sustainable and efficient construction of tricyclic and tetracyclic isoquinolones, avoiding a number of toxic waste/byproducts and metal contamination in the final products. The heterogeneous catalyst is stable and reusable up to 3 cycles and can be easily separated from the reaction mixture.

Conflicts of interest

There are no conflicts to declare.

Acknowledgements

Liangliang Song appreciates the Postdoctoral Mandate (PDM) of KU Leuven. This project has received funding from the European Union's Horizon 2020 Research and Innovation Programme under the Marie Skłodowska-Curie grant agreement no. 721290. This publication reflects only the author's view, exempting the Community from any liability. Project website: http://cosmic-etn.eu/. LVM thanks the Hercules Foundation for supporting the purchase of the diffractometer through project AKUL/09/0035. We acknowledge the FWO [Fund for Scientific Research-Flanders (Belgium)] and the Research Council of KU Leuven (BOF) for financial support. We acknowledge the support of RUDN University Program 5-100. The microscopy works have been conducted in the Laboratorio de Microscopias Avanzadas at Instituto de Nanociencia de Aragón-Universidad de Zaragoza. Authors acknowledge the LMA-INA for offering access to their instruments and expertise.

Notes and references

1 Z. Luo, A. W. Castleman and S. N. Khanna, *Chem. Rev.*, 2016, **116**, 14456.
2 E. C. Tyo and S. Vajda, *Nat. Nanotechnol.*, 2015, **10**, 577.
3 I. Chakraborty and T. Pradeep, *Chem. Rev.*, 2017, **117**, 8208.
4 (*a*) K. Kwak and D. Lee, *Acc. Chem. Res.*, 2019, **52**, 12; (*b*) T. V. W. Janssens, B. S. Clausen, B. Hvolbæk, H. Falsig, C. H. Christensen, T. Bligaard and J. K. Nørskov, *Top. Catal.*, 2007, **44**, 15.
5 (*a*) X. Kang and M. Zhu, *Chem. Soc. Rev.*, 2019, **48**, 2422; (*b*) M. Quijada, R. D. Muiño and P. M. Echenique, *Nanotechnology*, 2005, **16**, 176; (*c*) R. L. Johnston, *Philos. Trans. R. Soc., A*, 1998, **356**, 211.
6 A. Munir, K. S. Joya, T. Ulhaq, N.-U.-A. Babar, S. Z. Hussain, A. Qurashi, N. Ullah and I. Hussain, *ChemSusChem*, 2019, **12**, 1517.
7 R. R. Nasaruddin, T. Chen, N. Yan and J. Xie, *Coord. Chem. Rev.*, 2018, **368**, 60.
8 H. Häkkinen, *Chem. Soc. Rev.*, 2008, **37**, 1847.
9 T. Higaki, Y. Li, S. Zhao, Q. Li, S. Li, X.-S. Du, S. Yang, J. Chai and R. Jin, *Angew. Chem., Int. Ed.*, 2019, **58**, 8291.
10 K. Shimizu, K. Sawabe and A. Satsuma, *Catal. Sci. Technol.*, 2011, **1**, 331.

11 (*a*) O. S. Wenger, *J. Am. Chem. Soc.*, 2018, **140**, 13522; (*b*) W.-F. Lai, W.-T. Wong and A. L. Rogach, *Adv. Mater.*, 2020, **32**, 1906872.
12 X. Liu and D. Astruc, *Coord. Chem. Rev.*, 2018, **359**, 112.
13 P.-C. Chen, A. P. Periasamy, S. G. Harroun, W.-P. Wu and H.-T. Chang, *Coord. Chem. Rev.*, 2016, **320–321**, 129.
14 Y. Liu, D. Yao and H. Zhang, *ACS Appl. Mater. Interfaces*, 2018, **10**, 12071.
15 C. Coughlan, M. Ibáñez, O. Dobrozhan, A. Singh, A. Cabot and K. M. Ryan, *Chem. Rev.*, 2017, **117**, 5865.
16 Z. Wang, B. Chen and A. L. Rogach, *Nanoscale Horiz.*, 2017, **2**, 135.
17 Y. Lu, W. Wei and W. Chen, *Chin. Sci. Bull.*, 2012, **57**, 41.
18 M. R. Narouz, K. M. Osten, P. J. Unsworth, R. W. Y. Man, K. Salorinne, S. Takano, R. Tomihara, S. Kaappa, S. Malola, C.-T. Dinh, J. D. Padmos, K. Ayoo, P. J. Garrett, M. Nambo, J. H. Horton, E. H. Sargent, H. Häkkinen, T. Tsukuda and C. M. Crudden, *Nat. Chem.*, 2019, **11**, 419.
19 S. Zhao, R. Jin, H. Abroshan, C. Zeng, H. Zhang, S. D. House, E. Gottlieb, H. J. Kim, J. C. Yang and R. Jin, *J. Am. Chem. Soc.*, 2017, **139**, 1077.
20 C. N. Loynachan, A. P. Soleimany, J. S. Dudani, Y. Lin, A. Najer, A. Bekdemir, Q. Chen, S. N. Bhatia and M. M. Stevens, *Nat. Nanotechnol.*, 2019, **14**, 883.
21 H. Zhang, H. Liu, Z. Tian, D. Lu, Y. Yu, S. Cestellos-Blanco, K. K. Sakimoto and P. Yang, *Nat. Nanotechnol.*, 2018, **13**, 900.
22 Z.-Y. Wang, M.-Q. Wang, Y.-L. Li, P. Luo, T.-T. Jia, R.-W. Huang, S.-Q. Zang and T. C. W. Mak, *J. Am. Chem. Soc.*, 2018, **140**, 1069.
23 M. J. Alhilaly, R.-W. Huang, R. Naphade, B. Alamer, M. N. Hedhili, A.-H. Emwas, P. Maity, J. Yin, A. Shkurenko, O. F. Mohammed, M. Eddaoudi and O. M. Bakr, *J. Am. Chem. Soc.*, 2019, **141**, 9585.
24 K. Yonesato, H. Ito, H. Itakura, D. Yokogawa, T. Kikuchi, N. Mizuno, K. Yamaguchi and K. Suzuki, *J. Am. Chem. Soc.*, 2019, **141**, 19550.
25 T. Udayabhaskararao and T. Pradeep, *J. Phys. Chem. Lett.*, 2013, **4**, 1553.
26 X. Yuan, Z. Luo, Q. Zhang, X. Zhang, Y. Zheng, J. Y. Lee and J. Xie, *ACS Nano*, 2011, **5**, 8800.
27 X. Su and J. Liu, *ACS Appl. Mater. Interfaces*, 2017, **9**, 3902.
28 W. Wei, Y. Lu, W. Chen and S. Chen, *J. Am. Chem. Soc.*, 2011, **133**, 2060.
29 C. Vázquez-Vázquez, M. Bañobre-López, A. Mitra, M. A. López-Quintela and J. Rivas, *Langmuir*, 2009, **25**, 8208.
30 H. Kawasaki, Y. Kosaka, Y. Myoujin, T. Narushima, T. Yonezawa and R. Arakawa, *Chem. Commun.*, 2011, **47**, 7740.
31 N. Vilar-Vidal, M. C. Blanco, M. A. López-Quintela, J. Rivas and C. Serra, *J. Phys. Chem. C*, 2010, **114**, 15924.
32 (*a*) R. Manno, V. Sebastian, S. Irusta, R. Mallada and J. Santamaria, *Catal. Today*, 2021, **362**, 81; (*b*) J. Polte, *CrystEngComm*, 2015, **17**, 6809; (*c*) M. J. Ndolomingo, N. Bingwa and R. Meijboom, *J. Mater. Sci.*, 2020, **55**, 6195; (*d*) S. Biswas, J. T. Miller, Y. Li, K. Nandakumar and C. S. S. R. Kumar, *Small*, 2012, **8**, 688; (*e*) R. Manno, P. Ranjan, V. Sebastian, R. Mallada, S. Irusta, U. K. Sharma, E. V. Van der Eycken and J. Santamaria, *Chem. Mater.*, 2020, **32**, 2874.
33 (*a*) S. Chandrasekaran, S. Ramanathan and T. Basak, *AIChE J.*, 2012, **58**, 330; (*b*) S. Horikoshi, R. F. Schifmann, J. Fukushima and N. Serpone, *Microwave Chemical and Materials Processing: A Tutorial*, Springer Nature Singapore Pte Ltd, 2018; (*c*) I. R. Baxendale, J. J. Hayward and S. V. Ley, *Comb. Chem. High Throughput Screening*, 2007, **10**, 802.
34 J. P. Michael, *Nat. Prod. Rep.*, 2008, **25**, 139.
35 (*a*) J. P. Michael, *Nat. Prod. Rep.*, 2004, **21**, 625; (*b*) L. Li, W. W. Brennessel and W. D. Jones, *J. Am. Chem. Soc.*, 2008, **130**, 12414.
36 S. Y. Hong, J. Jeong and S. Chang, *Angew. Chem., Int. Ed.*, 2017, **56**, 2408.
37 Y. Fukui, P. Liu, Q. Liu, Z.-T. He, N.-Y. Wu, P. Tian and G.-Q. Lin, *J. Am. Chem. Soc.*, 2014, **136**, 15607.
38 L. Song, X. Zhang, G. Tian, K. Robeyns, L. Van Meervelt, J. N. Harvey and E. V. Van der Eycken, *Mol. Catal.*, 2019, **463**, 30.
39 W.-K. Luo, X. Shi, W. Zhou and L. Yang, *Org. Lett.*, 2016, **18**, 2036.
40 S. Zhou and R. Tong, *Chem.–Eur. J.*, 2016, **22**, 7084.
41 L. Song, G. Tian, Y. He and E. V. Van der Eycken, *Chem. Commun.*, 2017, **53**, 12394.
42 N. Quiñones, A. Seoane, R. García-Fandiño, J. L. Mascareñas and M. Gulías, *Chem. Sci.*, 2013, **4**, 2874.
43 X. Xu, Y. Liu and C.-M. Park, *Angew. Chem., Int. Ed.*, 2012, **51**, 9372.
44 N. K. Ojha, G. V. Zyryanov, A. Majee, V. N. Charushin, O. N. Chupakhin and S. Santra, *Coord. Chem. Rev.*, 2017, **353**, 1.
45 B.-H. Lee, C.-C. Wu, X. Fang, C. W. Liu and J.-L. Zhu, *Catal. Lett.*, 2013, **143**, 572.
46 A. W. Cook, Z. R. Jones, G. Wu, S. L. Scott and T. W. Hayton, *J. Am. Chem. Soc.*, 2018, **140**, 394.
47 (*a*) F. Wang, P. Chen and G. Liu, *Acc. Chem. Res.*, 2018, **51**, 2036; (*b*) Y. Wang, L. Deng, J. Zhou, X. Wang, H. Mei, J. Han and Y. Pan, *Adv. Synth. Catal.*, 2018, **360**, 1060; (*c*) M. Israr, H. Xiong, Y. Li and H. Bao, *Org. Lett.*, 2019, **21**, 7078; (*d*) F. Chen, S.-Q. Lai, F.-F. Zhu, Q. Meng, Y. Jiang, W. Yu and B. Han, *ACS Catal.*, 2018, **8**, 8925; (*e*) S. Mao, Y. Gao, X. Zhu, D. Guo and Y. Wang, *Org. Lett.*, 2015, **17**, 1692; (*f*) H. Xiao, H. Shen, L. Zhu and C. Li, *J. Am. Chem. Soc.*, 2019, **141**, 11440; (*g*) X. Yu, Q. Zhao, J. Chen, J. Chen and W. Xiao, *Angew. Chem., Int. Ed.*, 2018, **57**, 15505.
48 E. M. Johansson, M. A. Ballem, J. M. Córdoba and M. Odén, *Langmuir*, 2011, **27**, 4994.
49 E. M. Rivera-Muñoz and R. Huirache-Acuña, *Int. J. Mol. Sci.*, 2010, **11**, 3069.
50 E. M. Johansson, J. M. Córdoba and M. Odén, *Microporous Mesoporous Mater.*, 2010, **133**, 66.
51 S. Horikoshi and N. Serpone, *Microwaves in Catalysis: Methodology and Applications*, John Wiley & Sons, 2015.
52 (*a*) T. Udayabhaskararao, M. S. Bootharajua and T. Pradeep, *Nanoscale*, 2013, **5**, 9404; (*b*) M. S. Bootharaju, V. M. Burlakov, T. M. D. Besong, C. P. Joshi,

L. G. AbdulHalim, D. M. Black, R. L. Whetten, A. Goriely and O. M. Bakr, *Chem. Mater.*, 2015, **27**, 4289; (*c*) C. Zeng, T. Li, A. Das, N. L. Rosi and R. Jin, *J. Am. Chem. Soc.*, 2013, **135**, 10011.

53 Y. Du, H. Sheng, D. Astruc and M. Zhu, *Chem. Rev.*, 2020, **120**, 526.

54 (*a*) F. Ulusal, E. Erünal and B. Güzel, *J. Nanopart. Res.*, 2018, **20**, 219; (*b*) Y. Yang, C. Ochoa-Hernández, V. A. de la Peña O'Shea, J. M. Coronado and D. P. Serrano, *ACS Catal.*, 2012, **2**, 592; (*c*) S. Vajda and M. G. White, *ACS Catal.*, 2015, **5**, 7152.

55 (*a*) F. Morales-Lara, V. K. Abdelkader-Fernández, M. Melguizo, A. Turco, E. Mazzotta, M. Domingo-García, F. J. López-Garzón and M. Pérez-Mendoza, *J. Mater. Chem. A*, 2019, **7**, 24502; (*b*) C. García, S. Pollitt, M. van der Linden, V. Truttmann, C. Rameshan, R. Rameshan, E. Pittenauer, G. Allmaier, P. Kregsamer, M. Stöger-Pollach, N. Barrabés and G. Rupprechter, *Catal. Today*, 2019, **336**, 174; (*c*) L. Dien, T. Ishida, A. Taketoshi, D. Q. Truong, H. D. Chinh, T. Honma, T. Murayama and M. Haruta, *Appl. Catal., B*, 2019, **241**, 539.

56 F. Lin, X. Meng, E. Kukueva, T. Altantzis, M. Mertens, S. Bals, P. Cool and S. Van Doorslaer, *Dalton Trans.*, 2015, **44**, 9970.

57 P. Concepción, M. Boronat, S. García-García, E. Fernández and A. Corma, *ACS Catal.*, 2017, **7**, 3560.

58 T. Abiraman, K. Rajavelu, P. Rajakumar and S. Balasubramanian, *ACS Omega*, 2020, **5**, 7815.

59 Y. H. Lin, J. S. Ren and X. G. Qu, *Adv. Mater.*, 2014, **26**, 4200.

60 C. Liu, Y. Cai, J. Wang, X. Liu, H. Ren, L. Yan, Y. Zhang, S. Yang, J. Guo and A. Liu, *ACS Appl. Mater. Interfaces*, 2020, **12**, 42521.

61 J. Lian, Q. Liu, Y. Jin and B. Li, *Chem. Commun.*, 2017, **53**, 12568.

62 R. Ghosh, U. Goswami, S. S. Ghosh, A. Paul and A. Chattopadhyay, *ACS Appl. Mater. Interfaces*, 2015, **7**, 209.

63 L. Hu, Y. Yuan, L. Zhang, J. Zhao, S. Majeed and G. Xu, *Anal. Chim. Acta*, 2013, **762**, 83.